Title
T-cell activation is modulated by the 3D mechanical microenvironment

Authors
Majedi, Fatemeh S
Hasani-Sadrabadi, Mohammad Mahdi
Thauland, Timothy J
et al.

Publication Date
2020-09-01

DOI
10.1016/j.biomaterials.2020.120058

Peer reviewed

HHS Public Access

Author manuscript

Biomaterials. Author manuscript; available in PMC 2021 September 01.

Published in final edited form as:

Biomaterials. 2020 September ; 252: 120058. doi:10.1016/j.biomaterials.2020.120058.

T-cell activation is modulated by the 3D mechanical microenvironment

Fatemeh S. Majedi[1], **Mohammad Mahdi Hasani-Sadrabadi**[1], **Timothy J. Thauland**[2], **Song Li**[1], **Louis-S. Bouchard**[1,3], **Manish J. Butte**[2,4]

[1]Department of Bioengineering, University of California Los Angeles, Los Angeles, CA, 90095 USA

[2]Department of Pediatrics, Division of Immunology, Allergy, and Rheumatology, University of California Los Angeles, Los Angeles, CA, 90095 USA

[3]Department of Chemistry and Biochemistry, University of California Los Angeles, Los Angeles, CA, 90095 USA

[4]Department of Microbiology, Immunology, and Molecular Genetics, University of California Los Angeles, Los Angeles, CA, 90095 USA

Abstract

T cells recognize mechanical forces through a variety of cellular pathways, including mechanical triggering of both the T-cell receptor (TCR) and integrin LFA-1. Here we show that T cells can recognize forces arising from the mechanical rigidity of the microenvironment. We fabricated 3D scaffold matrices with mechanical stiffness tuned to the range 4-40 kPa and engineered them to be microporous, independently of stiffness. We cultured T cells and antigen presenting cells within the matrices and studied T-cell activation by flow cytometry and live-cell imaging. We found that there was an augmentation of T-cell activation, proliferation, and migration speed in the context of mechanically stiffer 3D matrices as compared to softer materials. These results show that T cells can sense their 3D mechanical environment and alter both their potential for activation and their effector responses in different mechanical environments. A 3D scaffold of tunable stiffness and

---

CEediT author statement

Fatemeh S. Majedi: Conceptualization, Investigation, Data Curation, Formal Analysis, Writing – Original Draft, Writing – Editing, Visualization

Mohammad Mahdi Hasani-Sadrabadi: Conceptualization, Investigation, Formal Analysis, Writing – Original Draft, Writing – Editing, Visualization

Timothy J. Thauland: Investigation, Writing – Editing

Song Li: Supervision, Writing – Original draft

Louis-S. Bouchard: Supervision, Writing – Original draft

Manish J. Butte: Project Administration, Formal Analysis, Visualization, Writing – Original draft, Writing – editing, Funding Acquisition, Supervision

Data availability

All data in the paper itself and supplemental figures. No restrictions on data availability.

Conflict of interest

The authors declare no conflicts of interest.

consistent microporosity offers a biomaterial advancement for both translational applications and reductionist studies on the impact of tissue microenvironmental factors on cellular behavior.

1. Introduction

When T cells recognize their cognate antigen on the surface of antigen presenting cells (APCs), they form a complex three-dimensional structure known as the immune synapse (IS) [1]. The IS, which facilitates communication between T cells and APCs via receptor-ligand interactions, is critical for T-cell activation, and constitutes a platform for the delivery of effector molecules (e.g. the contents of cytolytic granules). At the molecular level, receptor-ligand interactions at the IS trigger a series of signaling cascades. These TCR-proximal signals initiate transcriptional programs controlling T-cell proliferation, differentiation, and effector function.

The actin cytoskeleton is critical for T-cell biology, and pharmacological disruption of F-actin severely cripples T-cell motility, IS formation, and T-cell activation [2]. While cytoskeletal rearrangement is crucial for IS formation, the state of the cytoskeleton prior to T cell-APC conjugation is also important. We have previously shown that naive T cells are mechanically stiffer than activated effector T cells [3]. This difference in stiffness allows the more pliable effector T cells to form larger IS with APCs upon initial triggering, increasing the number of receptor-ligand interactions and enhancing activation. Thus, the T-cell cytoskeleton acts as a layer of regulation, allowing effector cells to sensitively respond to APCs. The stiffness of the antigen-presenting surface that T cells interact with also plays a role in activation. Experiments examining the interaction of T cells with stimulatory 2D surfaces of varying stiffnesses have demonstrated that relatively stiffer surfaces provide a stronger stimulus [4–9]. Elastic moduli around 15-20 kPa enable maximal spreading of T cells and optimal activation [10]. The cytotoxicity of T cells is also affected by substrate stiffness [11]. All these experiments have been performed in 2D, i.e., on surfaces.

While the mechanical properties of the T cell and the antigen-presenting surface have been investigated, the effect of the mechanical properties of the 3D microenvironment on actin-dependent T-cell functions such as motility, IS formation, and activation has barely been examined. The properties of 3D scaffolds can be manipulated by altering the density of polymers and crosslinkers. As cells migrate through scaffolds, they interact with functional groups that act as ligands for cell surface receptors, presented by the polymer. Thus, increasing polymer density results in a concomitant increase in ligand density and a decrease in mesh size, which alters cell-polymer interactions. On the other hand, keeping polymer content constant and varying the crosslinker density also alters the mesh size of the gel, which directly impacts molecular diffusion and cell motility [12]. While stiffness and ligand density can be modulated independently of polymer content with some synthetic polymers, the direct relationship between crosslinker density and mesh size has made it difficult at best to relate cell behavior to pure stiffness. Fortunately, in the case of the biodegradable polymer alginate gelation is induced by calcium ions. Due to the formation of G-blocks that provide pockets for calcium entrapment, the stiffness of the gel can be altered by varying the concentration of calcium ions without altering the ligand density or pore size.

Here we sought to mimic a range of biologically relevant stiffnesses that T cells experience while patrolling secondary lymphoid organs and peripheral tissues. We developed 3D porous alginate-based scaffolds that had similar rigidities to lymph nodes. Due to the unique characteristics that the alginate biopolymer possesses, we were able to modulate the rigidity of our scaffolds without affecting their porosity or ligand density. We used these scaffolds to study motility, proliferation, morphology, and immune synapse formation by T cells. We found that mechanically stiffer scaffolds enhanced T-cell activation in 3D cultures, akin to what has been observed for 2D substrates. Our morphological studies of T cells in hard and soft scaffolds revealed increased cell spreading in hard scaffolds. This effect likely contributes to the enhanced immune synapse size, activation, and proliferation we observed for cells cultured in stiff scaffolds.

2. Results and Discussion

2.1 Alginate-based matrix with constant microporosity with tunable elasticity.

To study how the mechanical stiffness of a 3D environment affects T-cell activation, proliferation, and IS formation, we developed a microporous, alginate-based, 3D scaffold (see Methods). To improve cell adhesion within these scaffolds, the alginate polymer was modified with RGD peptides. We screened polymers with a wide range of mechanical properties by titrating polymer and calcium concentration. Measurements of polymer stiffness demonstrated that we could modulate stiffness over two orders of magnitude by varying alginate density from 0.5% to 2.5% and calcium concentration from 10 mM to 60 mM (Fig. 1a). Gels with an order-of-magnitude difference in stiffness (4 and 40 kPa) in the range of biologically relevant tissues [13] were chosen for further study. To assess whether changing the stiffness altered the pore size, we acquired images of the microporous structure of our 3D gels by scanning electron microscopy (SEM) (Fig. 1b,c). We found that both the 40 and 4 kPa gels had a pore size of approximately 130 μm (Fig. 1d). These results reveal an ability to prepare 3D scaffolds of tunable stiffness and consistent microporosity.

2.2 T-cell motility within matrices

Given the importance of motility for T-cell function, we tracked T-cell migration in hard (40 kPa) and soft (4 kPa) gels using live-cell confocal microscopy. Fluorescently-labeled cells were seeded into gels and imaged over time crawling within the 3D scaffolds (Fig. 2a). Our analyses revealed that the average speed of T cells crawling within hard scaffolds (4.7 ± 0.3 μm/min, average ± 95% CI), was higher than within soft scaffolds (4.0 ± 0.2 μm/min) ($p < 1x10^{-5}$) (Fig. 2b). These speeds are in a biologically relevant range for T cells as seen in prior works ([14,15]). The ~20% higher speed of cells within stiffer scaffolds affords a higher probability of interaction between T cells and APCs. Thus, these findings are consistent with the fact that T cells were more activated and proliferative in the stiffer gels.

2.3 T-cell activation and effector functions within matrices

To examine the effect of 3D scaffold stiffness on CD4+ T-cell activation, we cultured T cells and monitored their proliferation. We seeded naive, CFSE-labeled CD4+ T cells purified from OT-II TCR transgenic mice plus peptide-loaded APCs into hard (40 kPa) and soft (4 kPa) 3D alginate scaffolds. To contrast 3D culture with conventional approaches, we

prepared 2D alginate-RGD gels with same mechanical stiffnesses as the 3D scaffolds (Supplemental Fig. 1). T cells and peptide-loaded APCs were placed onto these 2D substrates. Sequential generations of daughter cells result in roughly two-fold dilution of the CFSE dye when analyzed by flow cytometry. We also monitored the expression of the activation marker CD25 on the T cells. The stiffer substrate induced more proliferation in both 2D and 3D conditions than the softer substrate (Fig. 3a and b). Interestingly, the effect of stiffness on proliferation was greater in 3D scaffolds than on 2D surfaces (Fig. 3c and d). There were slightly more undivided cells in 3D conditions. We hypothesize that the increased degrees of freedom experienced by cells in a 3D matrix makes successful T cell-APC conjugation less frequent, and thus some T cells remained unactivated, as compared with crawling on a 2D surface. However, the proliferation index (a measure of the proliferative response of the cells that divided at least once) was higher in the stiff 3D environment (Fig. 3d). This result suggests that there is enhanced activation when T cells encounter an APC in 3D. In agreement with the proliferation data, upregulation of CD25, a cell-surface marker of T-cell activation, was more robust on stiffer substrates (Fig. 3e).

Effector responses of T cells can be assayed not only by proliferation and upregulation of activation markers like CD25, but also by production of key cytokines. To study whether cytokine expression is modulated by the mechanical microenvironment, we monitored the expression of IL-2, IFN-γ, and TNF-α in T cells cultured with peptide-pulsed APCs in 3D scaffolds of hard or soft stiffness by intracellular cytokine staining. We found that the percentage of cells that expressed these cytokines was higher in hard 3D scaffolds than those in softer scaffolds (Fig. 3f–h, isotype controls shown in Supplemental Fig. 2, example data in Supplemental Fig. 3). Moreover, in examining the single-cell amount of cytokine expressed in these responsive cells, the T cells responding to antigen in the stiffer matrix produced more effector cytokines than those in a softer matrix (Fig. 3i–k, example data in Supplemental Fig. 3). Some minor differences were noted in comparing cytokines elicited in 3D versus 2D. Notably, the expression of both TNF-α and IL-2 were higher in 2D than 3D. These results show that effector functions of T cells are augmented in stiffer 3D microenvironments as compared to softer environments.

2.4 T-cell activation with artificial APC microparticles within matrices

To better understand if the differential activation of T cells cultured in stiff and soft scaffolds above could have been indirect, i.e., arisen from the effects of stiffness upon the antigen presenting cells, we next examined the activation of T cells using artificial APC beads as the stimulus, which are unsusceptible to local micromechanics. We seeded microparticles fabricated from alginate and coated with anti-CD3 and anti-CD28 antibodies, as previously described [16], into the 3D scaffolds. As before we prepared 2D alginate-RGD gels with mechanical stiffnesses like the 3D scaffolds. We introduced naive, CFSE-labeled CD4+ T cells into the 3D scaffolds or onto the 2D substrates. For a few experiments, we introduced a third “medium” mechanical stiffness to offer an intermediate condition of 25 kPa. The stiffer substrate induced more proliferation and induced more of the activation marker CD25 than the softer one; the intermediate substrate was essentially the same as stiff (Fig. 4a–e). This result shows that there the enhanced activation of T cells encounter in stiff 3D scaffolds is independent of any mechanical effect of the APC.

As we did with real APCs, we studied whether cytokine expression by T cells is modulated by the mechanical microenvironment using the artificial APC microparticle beads. We found that the percentage of naïve T cells that expressed the effector cytokines was higher when activated in hard 3D scaffolds than those in softer scaffolds (Fig. 4f–h, example data in Supplemental Fig. 4). The single-cell amount of cytokines expressed in these T cells was greater in the stiffer matrix than in a softer matrix (Fig. 4i–k, example data in Supplemental Fig. 4) These results confirm that the augmentation of effector functions of T cells in stiffer 3D microenvironments as compared to softer environments is intrinsic to the T cell itself.

2.5 Immune synapses

Next, we studied the IS formed by T cells in our 3D alginate scaffolds and compared them to synapses formed on 2D hydrogels. We have previously shown that the size of the IS with antigen presenting cells correlates with T-cell activation [3]. The same has been shown when T cells interact with antibody-coated surfaces [10]. We seeded effector CD4+ T cells purified from spleens of OT-II TCR transgenic mice plus ovalbumin-loaded APCs into hard (40 kPa) and soft (4 kPa) 3D alginate scaffolds. To compare synapses formed in 3D with 2D, we prepared 2D alginate-RGD gels of the same mechanical stiffnesses. T cells and peptide-loaded APCs were placed onto these 2D substrates. As a control, we generated T cell-APC synapses by co-culturing them in pellet in a microtainer tube (see Methods). As a proxy for IS size, we measured the volume of the adhesion molecule LFA-1 that accumulated at the T cell-APC interface [3, 17]. LFA-1 plays a crucial role in IS formation [17], and is not expressed on the B cells that we used as APCs in these experiments, making it an ideal protein to define the extent of the T-cell IS [3]. We also stained the T cell-APC conjugates for the cytoskeletal protein F-actin. We found that immune synapses of T cells formed in stiff matrices (Fig. 5a–c) were significantly larger than those formed in soft matrices (Fig. 5d–f). There were no notable differences in the ultra-structural organization of actin and LFA-1 in the region of the IS in comparing T cells encountering APCs in stiff (Fig. 5g–i) and soft matrices (Fig. 5j–l). This finding held for T cells activated in 3D matrices or upon 2D substrates (Fig. 5m; 2D and control synapses shown in Supplemental Fig. 5). However, the IS formed under 3D conditions were significantly larger than those formed on 2D gels, offering a mechanistic explanation for the greater activation and proliferation seen in the prior experiments.

Because mechanosignaling through integrins has been the subject of many studies in lymphocytes and other cells, we sought to understand if the RGD peptide serving as an integrin ligand in our biomaterials was influencing T-cell activation. We prepared new stiff 3D matrices (~40 kPa) lacking RGD peptide and compared with those bearing RGD peptide. To eliminate any influence from integrin ligands on APCs, we used artificial APC beads as the stimulus for T cells, as above. We found that T cells were more activated in substrates bearing RGD peptide than those without (Supplemental Fig. 6). The T cells in an environment lacking RGD were even less activated than those cultured in soft 2D or 3D environments with RGD (c.f. Fig. 3b), despite the ample presence of stimulatory beads. This experiment suggests that T cell responses in 3D environments may lost if there is no tethering and/or ligation of integrins. Notably, the integrin signal provided by RGD here is coming in *trans* from the activation signal on beads, suggesting that T cells can integrate

signals from multiple distinct spatial sources. Mechanical tethering of ICAM-1, a major integrin ligand on APCs, has been shown to augment T cell activation through adhesive maturation of the integrin LFA-1 and signaling [18]. In addition, the impact of LFA-1 ligation has been well established as an important signal for polarization, clustering, activation, and effector activities of T cells [19–22], but disentangling the effects of these other signaling pathways versus mechanics was not attempted here.

Taken together, these results show that T cells have larger immune synapses with APCs, become more activated, and show more proliferation when encountering antigen in a mechanically stiff 3D microenvironment. Notably, the effector T cells in these experiments were previously, commonly activated before seeding into the various environments, and thus any differences in the subsequent interactions with APCs captured in these synapses were not due to differences in activation. Rather, we speculate these differences represent changes to the cytoskeletal adaptivity of T cells [3] due to the micromechanical environment.

3. Conclusion

In vivo, T cells are activated and carry out their effector functions in a 3D tissue environment comprising cells as well as polymeric matrices of collagen, hyaluronan and other polymers. However, the vast majority of *in vitro* experiments - which form the basis for much of our knowledge of T-cell biology - are carried out on plastic plates that are orders of magnitude stiffer than any biologically relevant substance. This practice continues even though it is accepted that the stiffness of the extracellular substrate affects the function of many different cell types [23]. Moreover, recent work has established that slow-moving cells like fibroblasts can sense time-dependent viscoelasticity independently from the elastic modulus of a substrate [24] and can even exploit viscoelasticity of materials to facilitate migration [25]. Whether this level of time-dependent mechanosensing occurs in highly motile cells like T cells has not been demonstrated.

Recently, several groups have demonstrated that the T-cell receptor itself senses mechanical forces through the development of a catch bond between the TCR and the pMHC [26]. Our group and others have further detailed the mechanical forces acting on the TCR to trigger activation [27,28]. We showed that the forces needed to trigger the TCR arise from the stereotypical pushing and pulling movements of the T cell itself after initial triggering. The pushing forces, when visualized at the cellular scale, are seen as an early, transient spreading of the contact area, allowing for greater contact between the T cell and APC in the immune synapse and enabling engagement of more TCRs [28,29]. When measured by AFM [28], micropillars [30], or traction force microscopy [8], the subsequent pulling forces generated by single T cells range from 100 pN to 1 nN. On the single-TCR level, these forces were found by DNA tension probes to range from 10-20 pN [31], which allows for identification of potent ligands and, subsequently, activation of the mechanosensing capability of the TCR. Mechanical contacts between the TCR the MHC, in addition to other key molecules like integrins and their ligands, support a nuanced view of TCR triggering that goes well beyond simple ligation and entails the actin cytoskeleton and a variety of signals [32].

The TCR is embedded in a fluid membrane buttressed by a complex cytoskeletal scaffold. Thus, anchoring of pMHC on a stiff substrate allows the TCR to experience a greater force when these molecules interact. Indeed a number of groups have investigated the role of anchoring TCR ligands on various substrate stiffnesses using 2D synthetic polymers such as PDMS and polyacrylamide [4,5,9]. Across many experimental modalities, the finding has been consistent: within the physiological range, the stiffer the anchoring, the greater the T-cell activation. Our work here is distinguished from these prior papers because our T cells were activated by antigen borne on antigen presenting cells rather than by antigen anchored directly to the stiff or soft substrate. These data could support the notion that the APC may convey some microenvironmental environmental information to T cells. Thus, to discern whether APC's role is paramount, we tested T-cell activation here using soft, artificial APC beads that are not influenced by the microenvironment, and T-cell activation was still augmented in the mechanically stiff 3D context as compared to the soft regime. Taken together, T cells can sense 3D environmental micromechanical stiffness whether the stimulatory signal comes from APC or artificial APC beads.

The mechanism by which T cells sense mechanics is as yet unclear; however, recent work supports a role for integrin signaling. Artificially increasing the tethering of the integrin ligand ICAM-1 on the APC side of the synapse facilitates activation of T cells, matures LFA-1, and influences the T-cell cytoskeleton [18,33]. Our own work here supports that integrin binding is important to mechanosensing in 3D. It is well known that the integrin LFA-1 on T cells binds to its ligand ICAM-1 on APCs. Anchoring of ICAM-1 to the APC cytoskeleton enhances the molecular forces acting on LFA-1, leading to the unfolding and "maturation" of the LFA-1 receptor into a higher affinity state for its ligand. Thus, forces acting on the T cell through the ICAM-1-LFA-1 system offer a route to co-stimulation that is independent of TCR triggering [18,34]. Another mechanism has been proposed to explain how mechanical stiffness is sensed through anchoring of LFA-1 by ICAM-1. Constrained, mature LFA-1 reduces the catalytic activity of the inhibitory phosphatase SHP-1 through interactions with the actin cytoskeleton and its centripetal flow [35]. Whether integrin signaling is paramount in mechanosensing is still unclear. Another route by which T cells could sense forces is through microenvironmental stiffness acting on their cytoskeleton or nuclear envelope [23,36]. This kind of mechanosensing would not act through the TCR or LFA-1, but rather through other intracellular sensors or through the cytoskeleton itself [37].

Optimal methods to exploit the mechanical properties of the 3D microenvironment on T-cell activation are lacking. A recent work showed that T cells sense differences between 2D and 3D collagen gels as well as high and low density 3D collagen gels, but this biomaterial unfortunately couples changes in stiffness with changes in porosity [38]. Another recent work compared 3D polystyrene mesh and Matrigel (a heterogeneous, nanoporous 3D matrix comprising collagens, laminin, proteoglycans and other ECM proteins) to 2D culture and found an enhancement in T-cell proliferation in 3D cultures [39]. 3D porosity has a major impact on motility and cytoskeletal regulation, and thus the use of Matrigel or collagen confounds studies of highly motile cells like T cells. Difficulties in tuning the stiffness of 3D biomaterials without dramatically altering their porosity has been a roadblock in pursuing a reductionistic understanding of the role of tissue mechanics [12]. Regardless, the potential scientific and clinical applications are compelling: encapsulation and therapeutic delivery of

T cells in hydrogels offers much potential for cancer immunotherapy and other adoptive cell therapies [40–42].

The development here of scaffolds of tunable stiffness and consistent microporosity thus represents an advance for T-cell biology. In summary, this work shows that T cells can sense their 3D mechanical environment.

4. Experimental Materials and Methods

4.1 Chemicals and Biologicals

Unless noted otherwise, all chemicals were purchased from Sigma-Aldrich, Inc. (St. Louis, MO). All glassware was cleaned overnight using concentrated sulfuric acid and then thoroughly rinsed with Milli-Q water. All the other cell culture reagents, solutions, and dishes were obtained from Thermo Fisher Scientific (Waltham, MA), except as indicated otherwise.

4.2 Scaffolds

To form the scaffolds, we first oxidized the alginate (Mw ~250 kDa, high G blocks; Novamatrix UP MVG, FMC Biopolymer, Rockland, Maine) with sodium periodate (1.5 %), overnight at room temperature, then quenched the reaction by dropwise addition of ethylene glycol for 45 min. We then dialyzed the solution (MWCO 3.5 kDa) against deionized water for 3 d followed by lyophilization. Afterward, the alginate was dissolved in MES (MES 150 mM, NaCl 250 mM, pH 6.5) and covalently conjugated to RGD-containing peptide (GGGGRGDY; GenScript USA Inc., Piscataway, NJ) using carbodiimide chemistry (NHS/EDC). The reaction was continued for 24 h followed by dialysis (MWCO 20 kDa) and lyophilization. This alginate-RGD complex in PBS was then cross-linked via calcium sulfate solution. The gels were casted in desired 24- or 96-well plates followed by two overnight washes to get rid of extra calcium ions and then used as 2D matrices. For 3D structures these same scaffolds were frozen at −80 °C, lyophilized for 3 d, and stored at 4 °C before cellular studies.

We prepared an array of different alginate formulations by varying either the polymer content or the amount of crosslinker (here $CaSO_4$). To measure the mechanical stiffness of our gels we used Instron 5542 mechanical tester and all the samples were tested at a rate of 1 mm/min. The Young's modulus was then calculated from the slope of the linear region that corresponds with 0–10% strain. The softer gel comprised alginate 1.25% with 10 mM $CaSO_4$. The medium gel comprised alginate 2.5% and 30 mM calcium. The stiffer gel comprised alginate 2.5% with 40 mM $CaSO_4$.

Scanning electron microscopy (SEM) images of the gels were taken to see the cross-sectional microstructure and porosity of the alginate-RGD scaffolds. The lyophilized scaffolds were freeze-fractured (using liquid nitrogen) for cross-sectional images. The scaffolds were sputtered with iridium (South Bay Technology Ion Beam Sputtering) prior to imaging with a ZEISS Supra 40VP scanning electron microscope (Carl Zeiss Microscopy GmbH). The sizes of pores from different parts of the SEM images were then measured and analyzed using ImageJ software (NIH).

Preparation and characterization of artificial APC microparticles—Alginate microparticles were formed using microfluidic platform according to our previous report [16]. Briefly, a mixture of alginate solution (1% w/v) and 4-arm PEG hydrazide (5 kDa, Creative PEG work, Chapel Hill, NC) (5 mM) was used as the inner aqueous phase. Mineral oil (plus 10 wt% Span 80) was used as the continuous phase. To form 4.5 μm alginate-based microparticles, 2 and 28 μL/min were used for the alginate and oil flows, respectively. Formed droplets were collected in a calcium bath (100 mM $CaCl_2$) and left at room temperature for 45 min for ionic crosslinking. The microgels were washed and centrifuged twice at 15,000 rpm for 10 min before further incubation in a solution containing hydroxybenzotriazole (HOBt) and 1-ethyl-3-(3-dimethylaminopropyl) carbodi-imide (EDC) for 2 h. Microparticles were then dialyzed against deionized water for three days to remove any residual and unreacted reagents, followed by freezing at −20 °C and lyophilization. Particles were then resuspended in deionized water for further use.

For the preparation of antibody-conjugated microparticles, anti-CD3 (clone 2C11; Bio-X-Cell) and anti-CD28 (clone 37.51; Bio-X-Cell) were covalently conjugated to the surface of particles using EDC/NHS chemistry. After activation of particle's carboxylic groups for 10 min, microparticles were washed with PBS twice and then antibodies were added to the particles and incubated under gentle stirring at 4 °C overnight. The protein-functionalized microparticles were then separated from the solution and washed several times. Unreacted functional groups were quenched by washing samples in Tris buffer (100 mM, pH 8). A 10-fold dilution of the conjugation density that is used in conventional plate-bound stimulation method for T-cell activation was picked as the final conjugation density for beads. Micro-BCA assay was used to quantify total amount of surface conjugated antibodies according to the manufacturer's protocol.

To immobilize beads to the scaffolds, the freeze-dried scaffolds were activated with EDC/NHS for 15 min. Then the scaffolds were washed twice with PBS (supplemented with 0.42 mM $CaCl_2$) before addition of 5×10^6 artificial APC microparticles. APC microparticles and scaffolds were then incubated at 4 °C for 4 h. Unbound microparticles were then washed away and 5×10^6 T cells were added to the scaffolds and cultured for 5 days to study their effector functions.

4.3 T-cell isolation and activation

All *in vitro* experiments were conducted in accordance with UCLA's institutional policy on humane and ethical treatment of animals following protocols approved by the Animal Research Committee. Five- to eight-week-old OT-II TCR transgenic mice (Jackson Labs) were used for all experiments. Cell-culture media was RPMI supplemented with 10% heat-inactivated FBS, 1% penicillin/streptomycin, 1% sodium pyruvate, 1% HEPES buffer, 0.1% μM 2-mercaptoethanol. CD4+ T cells were purified using negative selection enrichment kits (Stem Cell Technologies).

In vitro activation of CD4+ T cells was performed by culturing 1×10^6 cells/mL in tissue culture-treated 24-well plates that were pre-coated with anti-CD3 (clone 2C11; Bio X Cell) at a concentration of 10 μg/mL plus addition of 2 μg/mL soluble anti-CD28 (clone 37.51; Bio X Cell).

4.4 Immune synapses

To form *in vitro*, 2D or 3D immune synapses we used T cells from OT-II TCR transgenic mice (Jackson Labs) as above. T cells were extracted from spleens and CD4+ T cells were then purified using EasySep immunomagnetic negative selection (Stem Cell Technologies). Cells were then activated on plates as above. Effector T cells were then collected from wells and allowed to proliferate in interleukin-2 (IL-2, BRB Preclinical Repository, NCI, NIH)-containing medium (50 U/mL), prior to being used for experiments on days 3 to 5 of incubation. The I-A^b-bearing B-cell lymphoma line LB27.4 was purchased from the American Type Culture Collection and used as APCs for immune synapses. LB 27.4 cells were incubated with Ova peptide (1 μM) for several hours prior to co-culture with T cells.

For synapse formation on 2D or 3D hard vs. soft substrates.—Effector CD4+ T cells were mixed with antigen-pulsed APCs and then immediately seeded into 2D or 3D matrices. Then, for experiments in a 3D context, a mild centrifugation was performed to help with dispersion of the cells within the scaffolds and incubated at 37 °C for 30 min. Afterward, to evaluate just the synapses that were formed within the scaffold and not the ones that have been formed on the plastic bottom of the wells we physically transferred the scaffolds into new wells. Following transfer, they were fixed immediately with 4% PFA for 30 min. Then the gels were lysed using EDTA (50 mM) and alginate lyase (porcine, SigmaAldrich, 3.4 mg/mL). After digestion of the scaffold and recovery of the cells, followed by three centrifugation rounds to remove the dissolved polymer. Cells then were seeded on 8 well-plate Labtek II chamber pre-modified with Poly-D-lysine. The rest of staining and imaging are detailed below.

Control experiments.—A ratio of one peptide-pulsed LB27.4 APC cell to one T cell were mixed, followed by centrifugation for 1.5 min at 500 x *g* in a 1.5 mL Eppendorf microfuge tube. This pellet was then incubated at 37 °C for 15 min. Afterwards the pellet was gently pipetted and plated into 8-well Poly-D-lysine-coated Labtek II chambers. The chamber was then centrifuged for 1 min at 50 x *g*.

Staining and imaging.—The supernatant was removed from Labtek chambers, wells were washed once with PBS and fixed with 4% PFA. Then to permeabilize cells for intracellular staining, 0.1% Triton X-100 in PBS was incubated with cells for 5 min and blocked in 5% donkey serum for at least an hour. To stain the cells we used antibodies against LFA-1 (clone I21/7) and 4G10 with Alexa Fluor 568–conjugated phalloidin (Life Technologies) and DAPI. After several washes, wells were incubated with fluorescently conjugated secondary antibodies (Jackson ImmunoResearch). Eventually, samples were covered with Fluoromount-G with DAPI (eBioscience) and stored at 4 °C before imaging. For confocal imaging we used a 100× Plan Apo numerical aperture (NA) 1.4 objective (Nikon). Synapses were measured based on LFA-1 and actin accumulation at the T cell–APC interface as calculated in ImageJ/Fiji.

4.5 Flow cytometry

For flow cytometry analysis, antibodies to mouse CD4, CD25 (clone PC61.5), CD44 (clone IM7), were purchased from eBioscience, BioLegend, or BD Biosciences. To study

proliferation behavior of T-cell responses during various treatments their expansion was measured by 5-(and-6)-carboxyfluorescein diacetate, succinimidyl ester (CFSE) dilution. For CFSE dilution experiments, 5×10^5 naive CD4+ T cells were labeled with 2 μM CFSE for 13 min, followed by two washes and then incubation with splenocytes. Splenocytes were extracted from the spleen of wild type C57Bl/6 mice. Then the cells were incubated in ACK lysis buffer (Gibco) for 5 min at room temperature to remove red blood cells. The remaining cells were then treated with ova peptide as above to present to T cells. Trypan Blue was purchased from Calbiochem. Cells were analyzed on a Cytek DxP10 flow cytometer using FlowJo software (Treestar/BD).

For intracellular cytokine staining (ICCS), cells were fixed with cold 4% paraformaldehyde (PFA) for 20 min at room temperature and then permeabilized with 0.5% saponin for 10 min before blocking with PBS + 1% BSA + 5% donkey serum and staining with appropriate antibodies at 1:100 dilution. Cells were washed and analyzed by flow cytometry as above. The following antibodies were used for ICCS from Biolegend: IL-2 (clone JES6-5H3, APC, Cat #503808); TNF-α (clone MP6-XT22, PE, Cat #506313), IFN-γ (clone XMG1.2, BV421, Cat #505814); mouse IgG1 isotype control (clone MOPC-21, Cat #400112, Cat #400135); mouse IgG2a isotype control (clone MOPC-173, Cat #558055, Cat #558053).

4.6 Live-cell imaging

For the experiments regarding to the velocity measurement of T-cell migration on 2D gels or within 3D scaffolds, CD4+ T cells were stained with CellTrace CFSE (1 μM) as per the manufacturer's protocol (Life Technologies). The scaffold was mounted in a Delta T dishes (Bioptechs), which kept the media warmed to 37 °C. For experiments in presence of LB 27.4 cells as APCs, B cells were loaded with ovalbumin peptide prior to introduction to T cells and then seeded in matrices. Fields were imaged every 12 or 15 s for 10-20 min with a 40× Plan Fluor NA 0.6 extra-long working distance objective (Nikon). Imaris software (Bitplane/Oxford Instruments) was used to track CellTrace CFSE-loaded T cells over time. Velocities and other statistics were exported from Imaris and analyzed in R.

4.7 Statistical analysis

We employed permutation testing for all statistical comparisons including synapse size, proliferation, and activation markers. We used the permutationTest2 function of the "resample" package of R to calculate p values and determine the 95% confidence intervals, performing 50 to 100,000 permutations. Horizonal lines in all figures show the bootstrapped mean and boxes show the 95% confidence interval calculated from bootstrapping using the CI.t function of the "resample" package.

Supplementary Material

Refer to Web version on PubMed Central for supplementary material.

Acknowledgement

We acknowledge financial support from the NIH (R01 GM110482, R56 DE029157), the Jonsson Comprehensive Cancer Center (P30CA016042), and the UCLA Children's Discovery and Innovation Institute. We acknowledge the

support of the UCLA Molecular Biology Institute. The author would like to thank Sergey Mareninov and Dr. William Yong for their technical advice and help on the freeze-drying process.

References

[1]. Dustin ML, Visualization of cell-cell interaction contacts: Synapses and kinapses, Self. Nonself 2 (2011) 85–97. doi:10.4161/self.2.2.17931. [PubMed: 22299060]

[2]. Burkhardt JK, Carrizosa E, Shaffer MH, The actin cytoskeleton in T cell activation., Annu. Rev. Immunol 26 (2008) 233–59. doi:10.1146/annurev.immunol.26.021607.090347. [PubMed: 18304005]

[3]. Thauland TJ, Hu KH, Bruce MA, Butte MJ, Cytoskeletal adaptivity regulates T cell receptor signaling, Sci. Signal 3737 (2017) 1–11. http://stke.sciencemag.org/content/10/469/eaah3737 (accessed June 5, 2017).

[4]. Judokusumo E, Tabdanov E, Kumari S, Dustin ML, Kam LC, Mechanosensing in T lymphocyte activation, Biophys. J 102 (2012) L5–7. [PubMed: 22339876]

[5]. O'Connor RS, Hao X, Shen K, Bashour K, Akimova T, Hancock WW, Kam LC, Milone MC, Substrate rigidity regulates human T cell activation and proliferation., J. Immunol 189 (2012) 1330–9. [PubMed: 22732590]

[6]. Tabdanov E, Gondarenko S, Kumari S, Liapis A, Dustin ML, Sheetz MP, Kam LC, Iskratsch T, Micropatterning of TCR and LFA-1 ligands reveals complementary effects on cytoskeleton mechanics in T cells., Integr. Biol. (Camb) 7 (2015) 1272–84. doi:10.1039/c5ib00032g. [PubMed: 26156536]

[7]. Husson J, Chemin K, Bohineust A, Hivroz C, Henry N, Force generation upon T cell receptor engagement., PLoS One. 6 (2011) e19680. [PubMed: 21572959]

[8]. Hui KL, Balagopalan L, Samelson LE, Upadhyaya A, Cytoskeletal forces during signaling activation in Jurkat T-cells., Mol. Biol. Cell. 26 (2015) 685–95. doi:10.1091/mbc.E14-03-0830. [PubMed: 25518938]

[9]. Saitakis M, Dogniaux S, Goudot C, Bufi N, Asnacios S, Maurin M, Randriamampita C, Asnacios A, Hivroz C, Different TCR-induced T lymphocyte responses are potentiated by stiffness with variable sensitivity., Elife. 6 (2017) e23190. [PubMed: 28594327]

[10]. Wahl A, Dinet C, Dillard P, Nassereddine A, Puech P-H, Limozin L, Sengupta K, Biphasic mechanosensitivity of T cell receptor-mediated spreading of lymphocytes, Proc. Natl. Acad. Sci. U. S. A (2019) 1–6. doi: 10.1073/pnas.1811516116.

[11]. Basu R, Whitlock BM, Husson J, Le Floc'h A, Jin W, Oyler-Yaniv A, Dotiwala F, Giannone G, Hivroz C, Biais N, Lieberman J, Kam LC, Huse M, Cytotoxic T Cells Use Mechanical Force to Potentiate Target Cell Killing, Cell. 165 (2016) 100–110. doi:10.1016/j.cell.2016.01.021. [PubMed: 26924577]

[12]. Vining KH, Mooney DJ, Mechanical forces direct stem cell behaviour in development and regeneration., Nat. Rev. Mol. Cell Biol. 18 (2017) 728–742. doi: 10.1038/nrm.2017.108. [PubMed: 29115301]

[13]. Buxboim A, Ivanovska IL, Discher DE, Matrix elasticity, cytoskeletal forces and physics of the nucleus: how deeply do cells "feel" outside and in?, J. Cell Sci. 123 (2010) 297–308. doi:10.1242/jcs.041186. [PubMed: 20130138]

[14]. Bauer CA, Kim EY, Marangoni F, Carrizosa E, Claudio NM, Mempel TR, Dynamic Treg interactions with intratumoral APCs promote local CTL dysfunction, J. Clin. Invest 124 (2014) 2425–2440. doi:10.1172/JCI66375. [PubMed: 24812664]

[15]. Martinez GJ, Pereira RM, Aijo T, Kim EY, Marangoni F, Pipkin ME, Togher S, Heissmeyer V, Zhang YC, Crotty S, Lamperti ED, Ansel KM, Mempel TR, Lahdesmaki H, Hogan PG, Rao A, The Transcription Factor NFAT Promotes Exhaustion of Activated CD8+ T Cells, Immunity. 42 (2015) 265–278. doi:10.1016/j.immuni.2015.01.006. [PubMed: 25680272]

[16]. Majedi FS, Hasani-Sadrabadi MM, Thauland TJ, Li S, Bouchard L-S, Butte MJ, Augmentation of T-Cell Activation by Oscillatory Forces and Engineered Antigen-Presenting Cells., Nano Lett. (2019) 580704. doi:10.1021/acs.nanolett.9b02252.

[17]. Grakoui A, Bromley SK, Sumen C, Davis MM, Shaw AS, Allen PM, Dustin ML, The immunological synapse: a molecular machine controlling T cell activation., Science. 285 (1999) 221–7. http://www.ncbi.nlm.nih.gov/pubmed/10398592. [PubMed: 10398592]

[18]. Comrie WA, Li S, Boyle S, Burkhardt JK, The dendritic cell cytoskeleton promotes T cell adhesion and activation by constraining ICAM-1 mobility, J. Cell Biol. 208 (2015) 457–473. doi:10.1083/jcb.201406120. [PubMed: 25666808]

[19]. Dustin ML, Springer TA, Lymphocyte function-associated antigen-1 (LFA-1) interaction with intercellular adhesion molecule-1 (ICAM-1) is one of at least three mechanisms for lymphocyte adhesion to cultured endothelial cells., J. Cell Biol. 107 (1988) 321–31. doi:10.1083/jcb.107.1.321. [PubMed: 3134364]

[20]. Suzuki JI, Yamasaki S, Wu J, Koretzky GA, Saito T, The actin cloud induced by LFA-1-mediated outside-in signals lowers the threshold for T-cell activation, Blood. 109 (2007) 168–175. doi:10.1182/blood-2005-12-020164. [PubMed: 16973965]

[21]. Contento RL, Campello S, Trovato AE, Magrini E, Anselmi F, Viola A, Adhesion shapes T cells for prompt and sustained T-cell receptor signalling, EMBO J. 29 (2010) 4035–4047. doi:10.1038/emboj.2010.258. [PubMed: 20953162]

[22]. Sabatos CA, Doh J, Chakravarti S, Friedman RS, Pandurangi PG, Tooley AJ, Krummel MF, A synaptic basis for paracrine interleukin-2 signaling during homotypic T cell interaction., Immunity. 29 (2008) 238–48. doi:10.1016/j.immuni.2008.05.017. [PubMed: 18674934]

[23]. Discher DE, Janmey P, Wang Y-L, Tissue cells feel and respond to the stiffness of their substrate., Science. 310 (2005) 1139–43. doi:10.1126/science.1116995. [PubMed: 16293750]

[24]. Chaudhuri O, Gu L, Klumpers D, Darnell M, Bencherif SA, Weaver JC, Huebsch N, Lee HP, Lippens E, Duda GN, Mooney DJ, Hydrogels with tunable stress relaxation regulate stem cell fate and activity, Nat. Mater 15 (2016) 326–334. doi: 10.1038/nmat4489. [PubMed: 26618884]

[25]. Wisdom KM, Adebowale K, Chang J, Lee JY, Nam S, Desai R, Rossen NS, Rafat M, West RB, Hodgson L, Chaudhuri O, Matrix mechanical plasticity regulates cancer cell migration through confining microenvironments, Nat. Commun 9 (2018). doi:10.1038/s41467-018-06641-z.

[26]. Liu B, Chen W, Evavold BD, Zhu C, Accumulation of dynamic catch bonds between TCR and agonist peptide-MHC triggers T cell signaling, Cell. 157 (2014) 357–368. [PubMed: 24725404]

[27]. Kim ST, Takeuchi K, Sun Z-YJ, Touma M, Castro CE, Fahmy A, Lang MJ, Wagner G, Reinherz EL, The alphabeta T cell receptor is an anisotropic mechanosensor., J. Biol. Chem 284 (2009) 31028–37. [PubMed: 19755427]

[28]. Hu KH, Butte MJ, T cell activation requires force generation, J. Cell Biol. 213 (2016) 535–542. doi:10.1083/jcb.201511053. [PubMed: 27241914]

[29]. Negulescu PA, Krasieva TB, Khan A, Kerschbaum HH, Cahalan MD, Polarity of T cell shape, motility, and sensitivity to antigen., Immunity. 4 (1996) 421–30. [PubMed: 8630728]

[30]. Bashour KT, Gondarenko A, Chen H, Shen K, Liu X, Huse M, Hone JC, Kam LC, CD28 and CD3 have complementary roles in T-cell traction forces., Proc. Natl. Acad. Sci. U. S. A 111 (2014) 2241–6. doi:10.1073/pnas.1315606111. [PubMed: 24469820]

[31]. Liu Y, Blanchfield L, Ma VP-Y, Andargachew R, Galior K, Liu Z, Evavold B, Salaita K, DNA-based nanoparticle tension sensors reveal that T-cell receptors transmit defined pN forces to their antigens for enhanced fidelity., Proc. Natl. Acad. Sci. U. S. A 113 (2016) 5610–5. [PubMed: 27140637]

[32]. Blumenthal D, Burkhardt JK, Multiple actin networks coordinate mechanotransduction at the immunological synapse, J. Cell Biol. 219 (2020) 1–12. doi:10.1083/jcb.201911058

[33]. Jankowska KI, Williamson EK, Roy NH, Blumenthal D, Chandra V, Baumgart T, Burkhardt JK, Integrins modulate T cell receptor signaling by constraining actin flow at the immunological synapse, Front. Immunol 9 (2018) 1–19. doi:10.3389/fimmu.2018.00025. [PubMed: 29403488]

[34]. Comrie WA, Burkhardt JK, Action and Traction: Cytoskeletal Control of Receptor Triggering at the Immunological Synapse, Front. Immunol 7 (2016) 1–25. doi:10.3389/fimmu.2016.00068. [PubMed: 26834743]

[35]. Ben-Shmuel A, Joseph N, Sabag B, Barda-Saad M, Lymphocyte mechanotransduction: The regulatory role of cytoskeletal dynamics in signaling cascades and effector functions., J. Leukoc. Biol (2019) 1–13. doi: 10.1002/JLB.MR0718-267R.

[36]. Buxboim A, Irianto J, Swift J, Athirasala A, Shin J, Rehfeldt F, Discher DE, Coordinated increase of nuclear tension and lamin-A with matrix stiffness outcompetes lamin-B receptor that favors soft tissue phenotypes., Mol. Biol. Cell 28 (2017) 3333–3348. doi:10.1091/mbc.E17-06-0393. [PubMed: 28931598]

[37]. Totaro A, Panciera T, Piccolo S, YAP/TAZ upstream signals and downstream responses., Nat. Cell Biol. 20 (2018) 888–899. doi:10.1038/s41556-018-0142-z. [PubMed: 30050119]

[38]. Wang P, Dreger M, Madrazo E, Williams CJ, Samaniego R, Hodson NW, Monroy F, Baena E, Sanchez-Mateos P, Hurlstone A, Redondo-Munoz J, WDR5 modulates cell motility and morphology and controls nuclear changes induced by a 3D environment, Proc. Natl. Acad. Sci. U. S. A 115 (2018) 8581–8586. doi: 10.1073/pnas.1719405115. [PubMed: 29987046]

[39]. Perez Del Rio E, Martinez Miguel M, Veciana J, Ratera I, Guasch J, Artificial 3D Culture Systems for T Cell Expansion, ACS Omega. 3 (2018) 5273–5280. doi: 10.1021/acsomega.8b00521. [PubMed: 30023914]

[40]. Monette A, Ceccaldi C, Assaad E, Lerouge S, Lapointe R, Chitosan thermogels for local expansion and delivery of tumor-specific T lymphocytes towards enhanced cancer immunotherapies, Biomaterials. 75 (2016) 237–249. doi: 10.1016/j.biomaterials.2015.10.021. [PubMed: 26513416]

[41]. Stephan SB, Taber AM, Jileaeva I, Pegues EP, Sentman CL, Stephan MT, Biopolymer implants enhance the efficacy of adoptive T-cell therapy, Nat. Biotechnol 33 (2015) 97–101. doi:10.1038/nbt.3104. [PubMed: 25503382]

[42]. Smith TT, Moffett HF, Stephan SB, Opel CF, Dumigan AG, Jiang X, Pillarisetty VG, Pillai SPS, Wittrup KD, Stephan MT, Biopolymers codelivering engineered T cells and STING agonists can eliminate heterogeneous tumors, J. Clin. Invest 127 (2017) 2176–2191. doi:10.1172/JCI87624. [PubMed: 28436934]

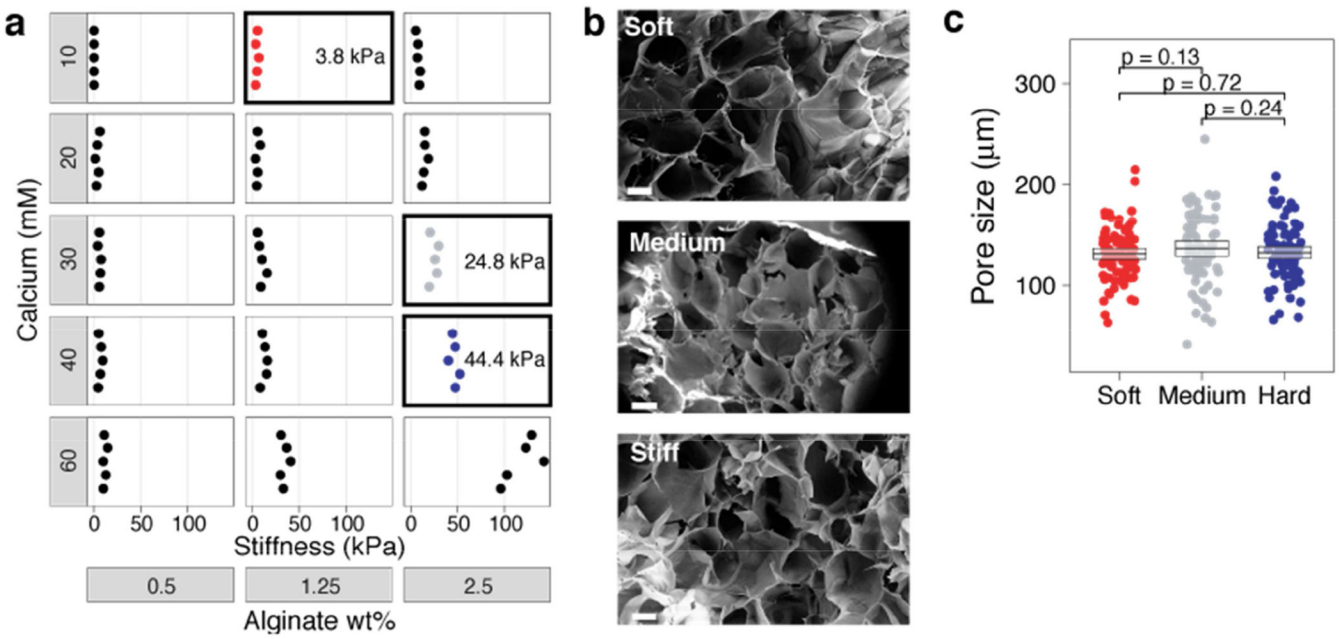

Fig. 1. Modulation of alginate gel stiffness without affecting porosity.

a, Different formulations of materials were screened by changing the concentration of the alginate polymer or calcium crosslinker. Stiffness values (Young's modulus) were measured on an Instron mechanical tester. Boxes are the soft, medium, and stiff conditions chosen for experiments in this paper. **b,** SEM images of three scaffolds with an order of magnitude difference in mechanical stiffness. Hard scaffolds were ~40 kPa, Medium scaffolds were ~25 kPa, and soft scaffolds were ~4 kPa. Images were taken from a region within the bulk of the scaffold. Scale bar is 100 µm. **c,** The size of at least 75 pores in each scaffold were measured from SEM images. Average pore sizes were 131.9 ± 6.1 µm for hard scaffolds, 136.1 ± 8.1 µm for medium scaffolds, and 130.9 ± 5.5 µm for soft scaffolds and were not significantly different. Bootstrap mean ± 95% CI shown (box).

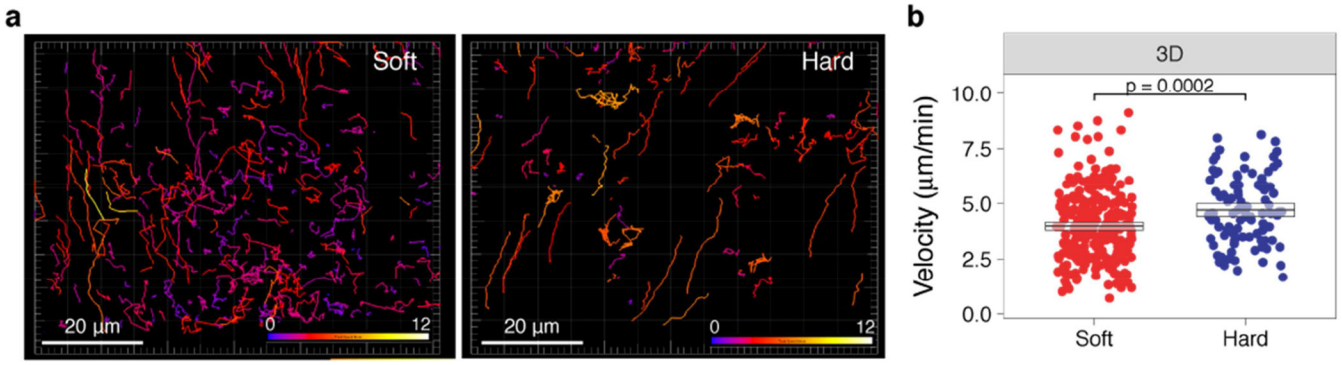

Fig. 2. T-cell motility is enhanced in stiff 3D scaffolds.

a, T cells crawling through microporous alginate scaffolds were imaged for 10 min. T-cell migration in soft (left) and stiff 3D scaffolds (right) were tracked with Imaris. Tracks are color-coded for average track velocity ranging from 0 to 12 μm/min. **b,** Mean velocity of cells crawling through soft and hard scaffolds. Each dot is the average track velocity of a single T cell. Bootstrapped mean and 95% CI are boxed.

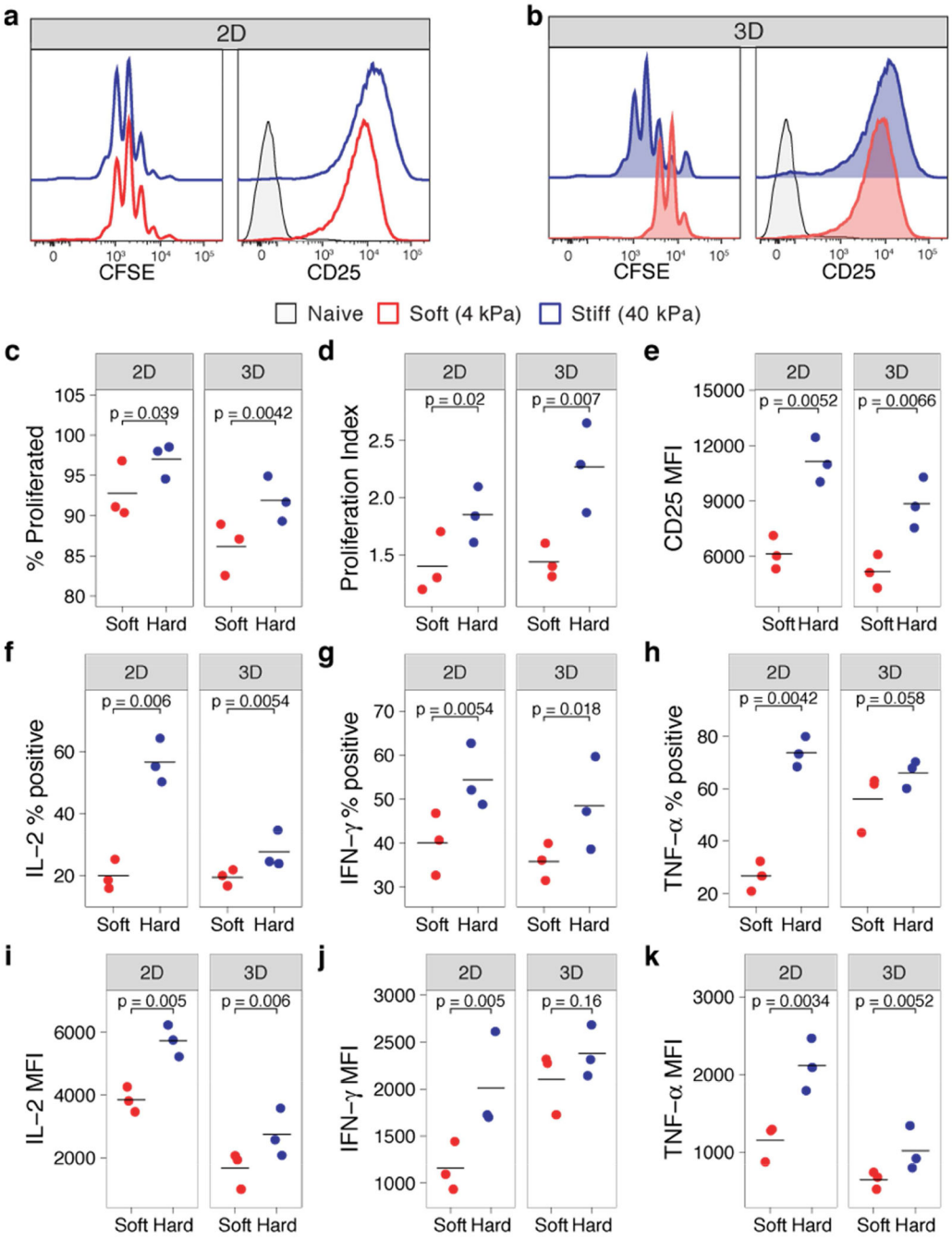

Figure 3. T-cell activation is modulated by the stiffness of 3D scaffolds.

(a and **b)** FACS analysis of CD25 expression and cell division (CFSE dilution) of CD4+ T cells co-cultured with peptide-pulsed APCs on 2D **(a)** or 3D **(b)** scaffolds with different stiffnesses. Cells were assayed at three days post-stimulation. **(c-e)** Percentage of cells that divided at least once **(c)**, proliferation index of divided cells **(d)**, and mean fluorescence intensity (MFI) of CD25 **(e)** are plotted for cells activated on 2D or 3D and stiff or soft scaffolds. **(f-h)** Percentage of T cells expressing the effector cytokines IL-2, IFN-γ, or TNF-

α. **(i-k)** Expression amount (MFI) of cytokines for those T cells making cytokines. Each dot represents one experiment.

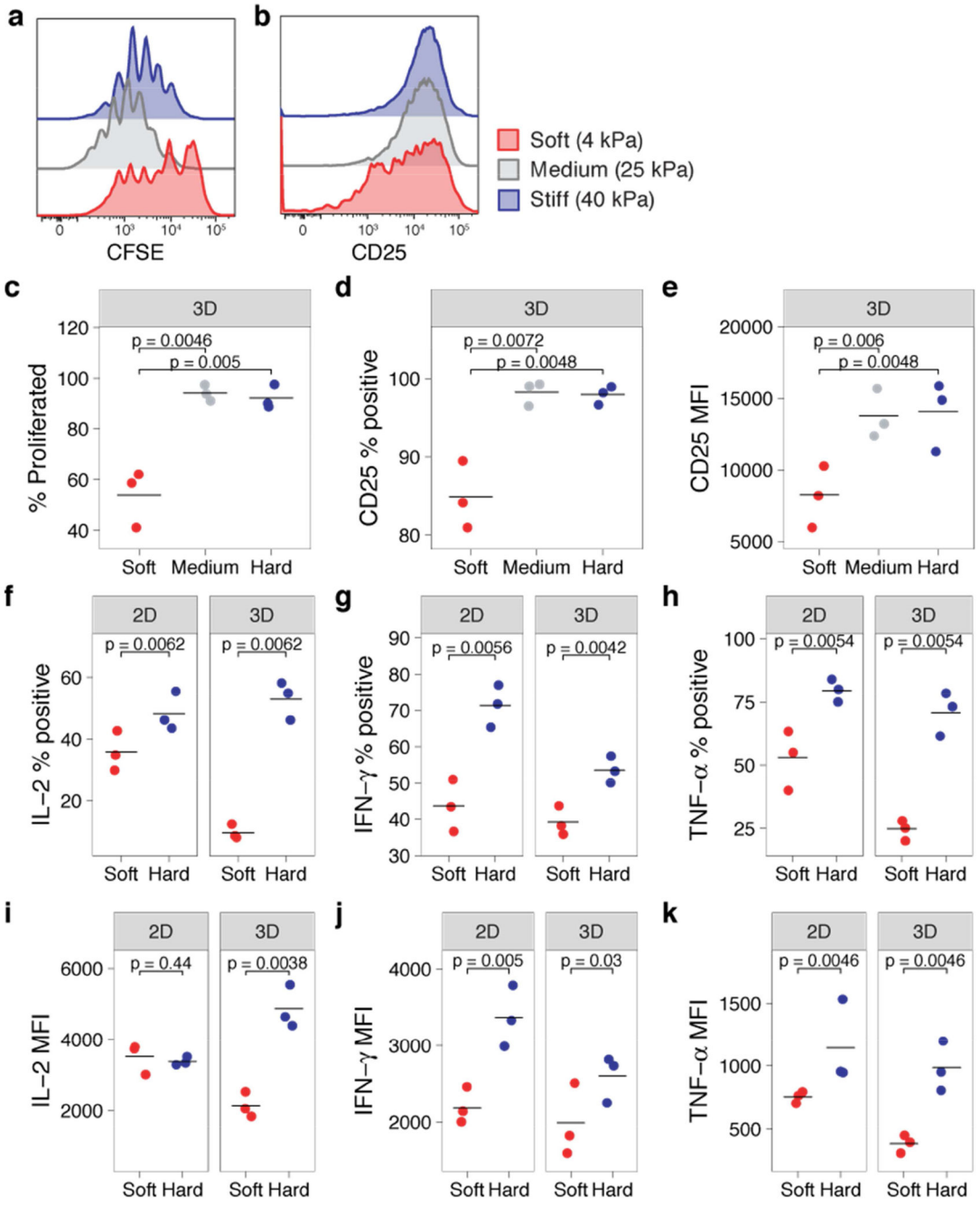

Figure 4. T-cell activation by microparticles is modulated by the stiffness of 3D scaffolds.

CD4+ T cells co-cultured with artificial APC microparticles on 2D **(a)** or in 3D **(b)** scaffolds with different stiffnesses. **(a** and **b)** FACS analysis of cell division (CFSE dilution) and CD25 expression assayed at three days post-stimulation. **(c)** Percentage of cells that divided at least once. **(d)** Percentage of T cells upregulating CD25 and **(e)** mean fluorescence intensity (MFI) of CD25. **(f-h)** Percentage of T cells expressing the effector cytokines IL-2, IFN-γ, or TNF-α. **(i-k)** Expression amount (MFI) of cytokines for those T cells making cytokines. Each dot represents one experiment.

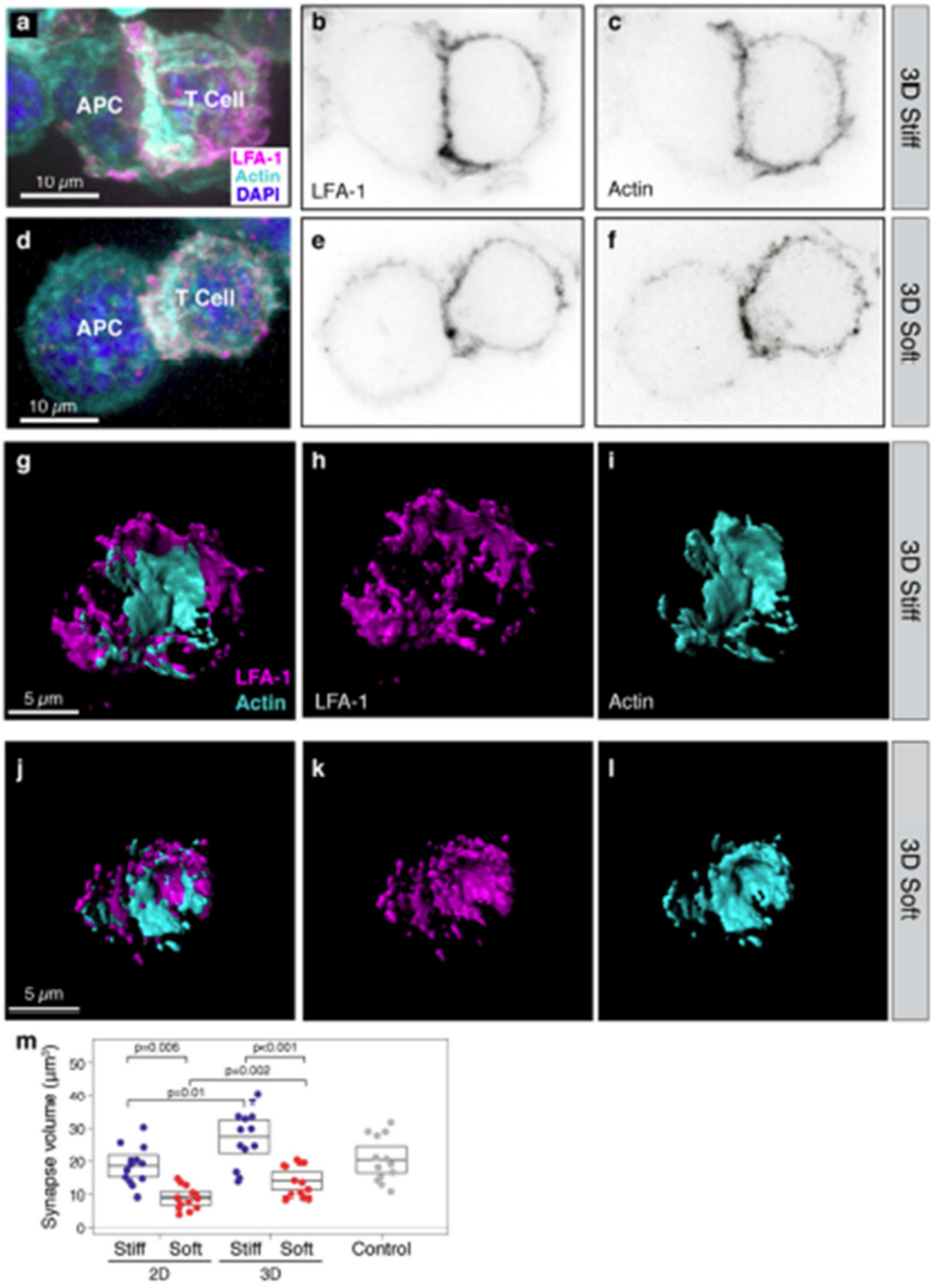

Figure 5. Immune synapse size is governed by the stiffness of 3D scaffolds.

(a-f) 3D confocal fluorescence microscopy examples of immune synapses formed by T cells and APCs seeded into **(a-c)** stiff (40 kPa) or **(b-f)** soft (4 kPa) 3D scaffolds. LFA-1 is magenta and F-actin is cyan. Cell nuclei were stained with DAPI (blue). Scale bar is 10 μm (for **a-f**). **(g-l)** Reconstructed 3D surfaces in Imaris showing images of LFA-1 and Actin in the formed IS in stiff **(g-i)** and soft **(j-l)** scaffolds. Colocalization of reconstructed 3D

surfaces given in **(g)** and **(j)**. **(m)** The volumes of LFA-1-positive voxels at T cell-APC interfaces were measured for IS formed under 2D or 3D conditions or control.